Tunneling from a correlated two-dimensional electron system transverse to a magnetic field

T. Sharpee and M. I. Dykman*

Department of Physics and Astronomy, Michigan State University, East Lansing, Michigan 48824

P. M. Platzman

Bell Laboratories, Lucent Technologies, Murray Hill, New Jersey 07974

We show that in a magnetic field parallel to a two-dimensional (2D) electron layer, strong electron correlations can change the rate of tunneling from the layer to the 3D continuum exponentially. It leads to a specific density dependence of the escape rate. The mechanism is a dynamical Mössbauer-type recoil, in which the Hall momentum of the tunneling electron is partly transferred to the whole electron system, depending on the interrelation between the rate of interelectron momentum exchange and the tunneling duration. We show that, in a certain temperature range, the parallel magnetic field can *enhance* rather than suppress the tunneling rate. The effect is due to the field induced energy exchange between the in-plane and out-of-plane motion. A parallel magnetic field can also lead to switchings between tunneling from different intra-well states, and between tunneling and thermal activation. Explicit results are obtained for a Wigner crystal. They are in qualitative and quantitative agreement with the relevant experimental data for electrons on helium, with no adjustable parameters. The theoretical results also suggest new experiments in semiconductor systems which will reveal electron correlations and their dynamical aspects.

I. INTRODUCTION

Many properties of low density two-dimensional electron systems (2DESs) are strongly influenced by electron correlations.[1–3] Tunneling is one of the most direct tools for revealing these correlations, as has been recently demonstrated in experiments on systems which display the quantum Hall effect.[4] In these experiments (see also Ref. 3) tunneling occurs between two 2D electron layers in a semiconductor heterostructure, which are separated by a high and narrow barrier. The tunneling current is then quite accurately determined by a constant (unknown) tunneling matrix element and the electron and hole propagators in the different layers, and is used to extract infromation about these propagators.

In this paper we consider a very different situation. The tunneling occurs from an interacting strongly correlated 2DES into a 3D continuum. The two are separated by a shallow and wide barrier. A magnetic field **B** is parallel to the electron layer (the results are readily generalized to the case of a tilted field). In this case the effect of the field on tunneling may not be described in terms of a phenomenological tunneling Hamiltonian: it is the tunneling matrix element itself that is sensitive to the electron correlations. As we show, it depends strongly, and very specifically, on electron density, and also on temperature and the magnetic field. This dependence tells us about the electron correlations and in-plane dynamics with frequencies comparable to the reciprocal imaginary tunneling time that an electron spends under the barrier. An exponentially strong deviation of the tunneling exponent in a magnetic field from the predictions of the single-electron theory have been observed for a 2DES on helium,[5] where the parameters are in the right range. However, the observations[5] until now have been unexplained. A theoretical framework for analysis of the problem at zero temperature was outlined in our recent communications.[6,7]

The physics of the effects we discuss relies on the fact that a magnetic field **B** parallel to a 2DES couples the out-of-plane tunneling motion of an electron to the in-plane motion. For an isolated electron, which is separated from the continuum by a 1D potential barrier $U(z)$, see Fig. 1, and is free to move in the plane (x,y), this results in an exponential suppression of the rate of tunneling decay. Indeed, when the electron moves by a distance z away from the layer, it acquires the in-plane Hall velocity $\mathbf{v}_H = (e/mc)\mathbf{B}\times\mathbf{z}$. The corresponding kinetic energy $mv_H^2/2 \equiv m\omega_c^2 z^2/2$ is subtracted from the energy of the out-of-plane tunneling motion ($\omega_c = |eB|/mc$ is the cyclotron frequency), or equivalently, there emerges a "magnetic barrier" $m\omega_c^2 z^2/2$. This leads to a sharp decrease of the decay rate.

The electron-electron interaction can totally change the above picture. If the electron system is spatially correlated, forming for example a Wigner crystal (WC), see Fig. 1, the tunneling electron transfers a part of its in-plane Hall momentum to other electrons.[7] This decreases the loss of the energy for out-of-plane tunneling motion.[8] The mechanism is similar to that of the Mössbauer effect where the momentum of a gamma quantum is given to the crystal as a whole.
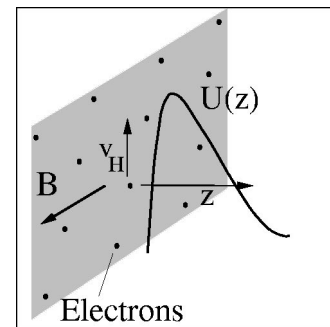

FIG. 1. The geometry of tunneling from a correlated 2DES transverse to a magnetic field.
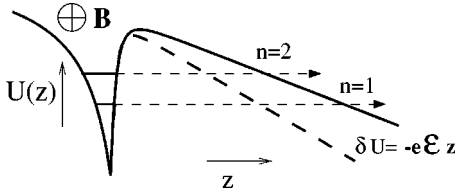
64 245309-1

FIG. 2. Magnetic field induced lowering of the tunneling barrier by thermal in-plane motion (schematically; the lowering is superimposed on the magnetic barrier for $T=0$). The effective electric field $\mathcal{E}$ is determined by the T-dependent optimal in-plane velocity, $\mathcal{E}=\mathbf{v}_{\mathrm{opt}}\times\mathbf{B}/c$.

However, in the present case the *dynamics* of the interelectron momentum exchange is very substantial. The characteristic momentum exchange rate is given by the zone-boundary plasma frequency ω_p, which is related to the electron density n by $\omega_p=(2\pi e^2 n^{3/2}/m)^{1/2}$. If ω_p exceeds the reciprocal duration of underbarrier motion in imaginary time τ_f^{-1} and ω_c, the WC momentum adiabatically follows that of the tunneling electron. As a result, the Hall velocity is nearly the same for all electrons, and $v_H\propto 1/N\to 0$ (N is the number of electrons). The effect of the magnetic field on tunneling is then compensated. For $\omega_p\tau_f\sim 1$ only partial compensation occurs. One can say that tunneling is accompanied by creation of phonons of the WC, and the associated energy goes towards the magnetic barrier. However, the barrier turns out to be smaller than for a free electron, and the tunneling rate is then exponentially larger. Still, for $T=0$ it is much smaller than the $B=0$ rate.

We show in this paper, that unexpectedly, in a certain temperature range the B-induced suppression of the rate of tunneling from a 2DES may be reversed, and then the decay rate exponentially increases with B. This happens because thermal energy of the in-plane electron motion is transferred by the magnetic field into the energy of tunneling motion. One can say that the in-plane motion with a velocity $\mathbf{v}$ changes the tunneling barrier by adding an effective out-of-plane electric field $c^{-1}\mathbf{v}\times\mathbf{B}$, as illustrated in Fig. 2. For an appropriate direction of $\mathbf{v}$ the field pulls an electron from the layer, and only these velocity directions contribute to the thermal-averaged tunneling rate.

The crossover from suppression to enhancement of tunneling by the field occurs for a certain temperature T_{cr}. It can be estimated by noticing that, for $B=0$, the tunneling rate from the ground state $W_0\propto\exp[-2S_0]$ exponentially depends on the energy E_g of the intrawell electron motion transverse to the layer [S_0 is the mechanical action for underbarrier motion; in what follows we use units where $\hbar=k_B=1$]. The derivative $\tau_0=\partial S_0/\partial E_g$ gives the imaginary duration of the underbarrier motion. The magnetic field effectively transfers the in plane electron energy E_{plane} into the out-of-plane energy E_g, at least in part. The probability to have an energy E_{plane} is $\propto\exp(-E_{\mathrm{plane}}/T)$. Therefore the overall probability, which is determined by the product of the two exponentials, depends on the interrelation between T and τ_0, and one may expect that $T_{\mathrm{cr}}\sim\tau_0^{-1}$.

The time τ_0 also often determines the temperature T_a for which there occurs a crossover from tunneling decay to de-cay via activated overbarrier transitions for $B=0$.[9,10] Therefore T_a and T_{cr} are of the same order of magnitude. The interrelation between these temperatures is determined by the parameters of the system, and various interesting situations may occur depending on these parameters, as we discuss below. For example, the logarithm of the escape rate may increase with B even for $T>T_a$, because in a certain B range, the rate of tunneling from the ground state exceeds the activation rate, even though it is smaller than the activation rate for $B=0$. Similarly, with increasing B there may occur switching from tunneling from the excited intrawell states (see Fig. 2) to tunneling from the ground state.

For $T<T_{\mathrm{cr}}$, on the other hand, the tunneling rate decreases with the increasing B. For large enough B the tunneling rate becomes smaller than the rate of activated escape, which then determines the overall escape rate.

Although the thermal B-induced tunneling enhancement is generic, as we show it arises only in systems where intrawell motion transverse to the layer is not semiclassical. This is typical for 2DESs, where the confining potential $U(z)$ is usually nonparabolic near the minimum, and even nonanalytic, with a step in the case of heterostructures and, in the case of electrons on helium, the singularity of the image potential. In contrast, the enhancement does not arise[11] if the tunneling rate can be found using the instanton (bounce) technique.[12] This technique is traditionally applied to describe tunneling for $B=0$. For $B\neq 0$, it has to be modified, because the magnetic field breaks time-reversal symmetry, and therefore, except for the case where the Hamiltonian of the system has a special form,[13] there are no escape trajectories in real space and imaginary time.[14]

In what follows, explicit results on the effect of electron correlations on tunneling are obtained assuming that electrons form a Wigner crystal. Because of strong correlations, overlapping of the wave functions of individual electrons is small, and electrons can be "identified." The problem is then reduced to the tunneling of an electron coupled to in-plane vibrations of the Wigner crystal. As we show, the results provide a good approximation also for a correlated electron liquid.

In Sec. II we formulate the model. In Sec. III we provide a general expression for the tunneling rate in the WKB approximation, with account taken of the discreteness of the energy spectrum of electron motion transverse to the layer. The result can be understood in terms of the tunneling trajectory where the duration of motion transverse to the layer (in imaginary time) depends on temperature and the magnetic field in a nontrivial way. The actual derivation is given in the Appendix. We then analyze the tunneling exponent, including the cases of $T=0$ and of finite T but small frequencies of electron vibrations. In Sec. IV we discuss temperature effects and show the possibility of B-induced enhancement of tunneling and of switching between different regimes of escape from the potential well. In Sec. V explicit results are obtained using the Einstein model of the Wigner crystal in which all phonons are assumed to have the same frequency. Closed-form expressions are obtained for a triangular and square tunneling barriers. In Sec. VI we apply the results to electron tunneling from helium surface and provide a de-

tailed comparison with the experimental data.[5] Section VII contains concluding remarks.

II. TUNNELING FROM A HARMONIC WIGNER CRYSTAL

A 2D electron system displays strong correlations if the ratio Γ of the characteristic Coulomb energy of the electron-electron interaction $e^2(\pi n)^{1/2}$ to the characteristic kinetic energy is large (here, n is the electron density). In degenerate systems the kinetic energy is the Fermi energy $\pi n/m$, whereas in nondegenerate systems it is the thermal energy T. An example of a strongly correlated nondegenerate 2DES is electrons on helium. The experimental data for this system refer to the range $\Gamma > 20$.[2] A classical transition to a Wigner crystal (WC) was observed for $\Gamma \approx 130$.[15,16] Recently much attention have attracted also strongly correlated low-density electron and hole systems in semiconductors, where there have been reached the values of $\Gamma \sim 40$ which are expected to be sufficient for Wigner crystallization in a degenerate system.[1] Another example is strongly correlated systems in the quantum Hall regime.

In what follows we discuss the effect on tunneling only of the magnetic field **B** parallel to the electron layer. It is most pronounced if the tunneling length L is long, because the in-plane Hall momentum due to tunneling $m\omega_c L$ is simply proportional to L. Respectively, of utmost interest to us are systems with broad and comparatively low barriers. Yet in experimental systems the barrier widths are most likely to be less than 10^3 Å. Therefore, in order to somewhat simplify the analysis we will assume that L is less than the average interelectron distance $\sim n^{-1/2}$. In this case, since electrons in a strongly correlated system stay away from each other, the in-plane electron dynamics only weakly affects the tunneling potential.[17] We will neglect this effect for $B=0$.

The major effect on tunneling for $B \neq 0$ should come from recoil from a few nearest neighbors, or alternatively, from short-wavelength in-plane excitations which have large density of states. The presence or absence of long-range order in the 2DES does not then affect the tunneling rate, see Sec. III B. Therefore we will analyze tunneling assuming that the electron system is a Wigner crystal. As we show, the problem is then reduced to tunneling of a polaron formed by the electron coupled to phonons of the WC, with the coupling strength controlled by the magnetic field. We believe that this model contains the most essential physics of tunneling from correlated systems and therefore provides a good approximation even where electrons form a correlated fluid.

In a strongly correlated system, exchange effects are not significant, and one can identify the tunneling electron. Its out-of-plane motion for $B=0$ is described by the Hamiltonian

$$H_0 = \frac{p_z^2}{2m} + U(z). \tag{1}$$

The potential $U(z)$ has a well which is separated by a tunneling barrier from the extended states with a quasicontinuous spectrum, see Fig. 1. The well is nonparabolic near the minimum, in the general case. The metastable intrawell states are quantized. We will consider temperatures for which nearly all electrons are in the lowest level, with energy E_g.

The magnetic field **B** parallel to the layer mixes the out-of-plane motion of the tunneling electron with the in-plane vibrations of the Wigner crystal. The full Hamiltonian is of the form

$$H = H_0 + H_B + H_v, \tag{2}$$

with

$$H_v = \frac{1}{2} \sum_{\mathbf{k},j} [m^{-1}\mathbf{p}_{\mathbf{k}j}\mathbf{p}_{-\mathbf{k}j} + m\omega_{\mathbf{k}j}^2\mathbf{u}_{\mathbf{k}j}\mathbf{u}_{-\mathbf{k}j}] \tag{3}$$

and

$$H_B = \frac{1}{2}m\omega_c^2 z^2 - \omega_c z N^{-1/2}\sum_{\mathbf{k},j} [\hat{\mathbf{B}} \times \mathbf{p}_{\mathbf{k}j}]_z. \tag{4}$$

Here $\mathbf{p}_{\mathbf{k}j}$, $\mathbf{u}_{\mathbf{k}j}$, and $\omega_{\mathbf{k}j}$ are the 2D momentum, displacement, and frequency of the WC phonon of branch j ($j=1,2$) with a 2D wave vector **k**. We chose the equilibrium in-plane position of the tunneling electron to be at the origin. Then its in-plane 2D momentum is $\mathbf{p}=N^{-1/2}\Sigma\mathbf{p}_{\mathbf{k}j}$ for $B=0$.

The interaction Hamiltonian H_B (4) *does not* conserve the phonon quasimomentum **k**. The Hall momentum of the tunneling electron is transferred to the WC as a whole. The term H_B couples the out-of-plane motion to lattice vibrations. The problem of many-electron tunneling is thus mapped onto a familiar problem of a particle coupled to a bath of harmonic oscillators,[18,13] with the coupling strength controlled by the magnetic field. The distinctions from the standard situation stem from the nonparabolicity of the potential well near the minimum and from the fact that coupled by H_B are the electron *coordinate* z and the in-plane *momenta* of the lattice. These quantities have different symmetry with respect to time inversion. In the general case [for example, where the potential energy of the system has odd-order terms in the displacements $\mathbf{u}_{\mathbf{k}j}$], the broken time-reversal symmetry requires a special approach to the analysis of tunneling.[6] The results discussed below can be appropriately generalized using this approach.

For the model (2), the analysis is simplified by the structure of the Hamiltonian (see Ref. 13). For vibrations with the Hamiltonian H_v (3), one can make a canonical transformation from the canonical coordinates and momenta $\mathbf{u}_{\mathbf{k}j}$ and $\mathbf{p}_{\mathbf{k}j}$ to the new canonical coordinates and momenta $\mathbf{p}_{\mathbf{k}j}$ and $-\mathbf{u}_{\mathbf{k}j}$, respectively. This transformation interchanges the time-reversal symmetry of the in-plane dynamical variables, it makes $\mathbf{p}_{\mathbf{k}j}$ and $\mathbf{u}_{\mathbf{k}j}$ even and odd in time, respectively. Because H_B is independent of $\mathbf{u}_{\mathbf{k}j}$ and is linear in $\mathbf{p}_{\mathbf{k}j}$, in the new variables it takes on a more familiar form of a "potential" coupling which depends on the dynamical coordinates z, $\mathbf{p}_{\mathbf{k}j}$ only, with restored time-reversal symmetry.

III. THE TUNNELING EXPONENT

A. General formulation

We now evaluate the escape rate W in the WKB approximation. The major emphasis will be placed on the tunneling exponent. We will assume that the escape rate is much less than the intrawell relaxation rate, and the distribution over the intrawell states of the system is thermal. This is not necessarily true for 2D systems. Usually the in-plane degrees of freedom (phonons) equilibrate fast, but the distribution over the states $n = 1,2,3,\ldots$, of quantized intrawell motion in the z direction requires longer time to become equilibrium. Our results can be generalized to the case of slow intrawell relaxation, see Sec. VI.

The rates of tunneling decay of intrawell states sharply increase, whereas the thermal state population decreases with the state energy. As a result, there is a comparatively small group of states (generally with the same n but with different phonon occupation numbers), from which the system is most likely to escape. To logarithmic accuracy

$$W \propto Z_e^{-1} \max_n \exp(-R_n - \beta E_n),$$
$$R_n = \min_{z(\tau)} \mathcal{R}_n[z(\tau)]. \tag{5}$$

Here, R_n is the tunneling exponent for the nth state, and the factor $\exp(-\beta E_n)$ allows for thermal occupation of this state ($\beta \equiv 1/k_B T$). The factor $Z_e \approx \exp(-\beta E_1)$ is the partition function for the motion transverse to the layer in the neglect of tunneling.

Equation (5) is obtained by statistical averaging over phonons, for each state n, as described in the Appendix. It differs from the standard procedure,[12] because the intrawell motion in the z direction is not semiclassical. Even though the underbarrier motion is semiclassical, its duration in imaginary time τ_f is not equal to $\beta/2$. Nevertheless the result of elimination of phonons, obtained by solving the linear equations of underbarrier motion (A6) for the phonon "coordinates" $\mathbf{p}_{\mathbf{k}j}(\tau)$ has a familiar form of an influence functional.[18] In fact, the effective duration of the phonon tunneling motion is still equal to $\beta/2$, see Eq. (A14). As a result R_n is given by R_α (A13) [$\alpha = \{n, n_{\mathbf{k}j}\}$] with the appropriate phonon occupation numbers $n_{\mathbf{k}j}$.

Overall, $\mathcal{R}_n[z]$ in Eq. (5) is a retarded action functional for a 1D electron motion normal to the layer

$$\mathcal{R}_n[z] = \int_0^{2\tau_f} d\tau_1 \left[\frac{m}{2}\dot{z}^2 + U(z) + \frac{1}{2}m\omega_c^2 z^2(\tau_1) \right]$$
$$- 2\tau_f E_n + \mathcal{R}_{ee}[z]. \tag{6}$$

The first two terms here give the action for underbarrier motion of an electron in the magnetic field, whereas $\mathcal{R}_{ee}$ gives the retarded action which results from the electron-electron interaction

$$\mathcal{R}_{ee}[z] = -\frac{1}{2}\omega_c^2 \int_0^{2\tau_f} \int_0^{\tau_1} d\tau_1 d\tau_2 z(\tau_1) z(\tau_2) \chi(\tau_1 - \tau_2). \tag{7}$$

Here, $\chi(\tau) = \langle \mathbf{p}_\parallel(\tau)\mathbf{p}_\parallel(0) \rangle$ is the correlation function of the in-plane momentum $\mathbf{p}_\parallel$ of an electron in the correlated 2DES. For electrons forming a Wigner crystal, $\chi(\tau)$ is simply related to the phonon Green's function

$$\chi(\tau) = \frac{m}{2N} \sum_{\mathbf{k}j} \omega_{\mathbf{k}j}[(\bar{n}_{\mathbf{k}j} + 1)e^{-\omega_{\mathbf{k}j}\tau} + \bar{n}_{\mathbf{k}j}e^{\omega_{\mathbf{k}j}\tau}] \tag{8}$$

($\bar{n}_{\mathbf{k}j} = [\exp(\beta\omega_{\mathbf{k}j}) - 1]^{-1}$ is the thermal occupation number).

The extreme tunneling trajectory $z(\tau)$, which provides a minimum to the functional $\mathcal{R}_n$, goes from a point $z = z_{\text{in}}$ near the well to the boundary of the classically accessible region over the time τ_f, and then bounces back to the point z_{in} [in Eq. (6) we set $z_{\text{in}} = 0$]. The initial point z_{in} is chosen under the barrier, but close to the well, so that the wave function is semiclassical and the out-of-plane electron motion is separated from the in-plane vibrations, see the Appendix. Therefore the initial condition for the tunneling trajectory have the same form as for a free electron

$$z(0) = z_{\text{in}}, \quad \dot{z}(0) = \frac{\gamma_n}{m} = \left[\frac{2[U(z_{\text{in}}) - E_n]}{m} \right]^{1/2}. \tag{9}$$

Here, γ_n is the characteristic decrement of the intrawell wave function in the z direction.

The duration of tunneling motion τ_f has to be obtained from the condition at the boundary of the classically accessible range behind the barrier. If the potential $U(z)$ is smooth there, the matching of the WKB wave functions occurs at a turning point[19]

$$\dot{z}(\tau_f) = 0. \tag{10}$$

The tunneling trajectory is by construction symmetrical in time with respect to τ_f, $z(\tau_f + \tau) = z(\tau_f - \tau)$ for $0 < \tau < \tau_f$.

We expect that not only do Eqs. (6), (7) apply to a Wigner crystal, but they also provide a good approximation in the case of a correlated electron liquid, and then Eq. (7) corresponds to the lowest-order term in the cumulant expansion of the appropriate propagator. Parallel magnetic field couples the tunneling motion of an electron to the in-plane dynamical degress of freedom of all other electrons. Tunneling provides a way to measure the actual autocorrelation function of the in-plane momentum.

The term $\mathcal{R}_{ee}$ is negative. It means that the electron-electron interaction in a correlated 2DES always *increases* the tunneling rate in the presence of a magnetic field. Moreover, when this term exceeds $(m\omega_c^2/2)\int z^2 d\tau$, the tunneling exponent as a whole decreases with the increasing B.

Two physical phenomena are described by the term $\mathcal{R}_{ee}$. One is the dynamical compensation of the Hall momentum of the tunneling electron by the WC as the electron moves under the barrier in the z direction. The other is thermal "preparation" of the Hall momentum, which is then transformed by the magnetic field into the momentum of motion in the z direction. We analyze these effects in the following subsections.

B. Zero temperature limit

It would be natural to think that, since tunneling is accompanied by creation of phonons for $T=0$, then the higher the phonon frequency the lower the tunneling rate. In fact just the opposite is true.

The effect of the electron-electron interaction on tunneling, as characterized by $\mathcal{R}_{ee}$, depends on the interrelation between the characteristic phonon frequency ω_p and the tunneling duration τ_f. When the tunneling electron is "pushed" by the Lorentz force, it exchanges the in-plane momentum with other electrons. The parameter $\omega_p\tau_f$ determines what portion of the momentum goes to the crystal as a whole during the tunneling (note that the tunneling motion goes in imaginary time; a discussion of the physical meaning of the tunneling duration is given in Ref. 20). As mentioned in the Introduction, in the adiabatic limit of large $\omega_p\tau_f$, all electrons have same in-plane velocity, with an accuracy to quantum fluctuations. Therefore the Lorentz force produces no acceleration, and *no phonons* are created during the tunneling. The effect of the magnetic field on tunneling should then be eliminated.

These arguments are confirmed by the analysis of Eq. (7). If the electron system is rigid enough in the plane, so that $\omega_{\mathbf{k}j}\tau_f\gg1$, the major contribution to $\mathcal{R}_n$ comes from $\tau_1-\tau_2 \sim \omega_{\mathbf{k}j}^{-1}\ll\tau_f$. Therefore $z(\tau_2)\approx z(\tau_1)$, so that in $\mathcal{R}_n$ the two terms $\propto\omega_c^2$ compensate each other. The tunneling occurs as if the electron were disconnected from the phonons and did not experience a magnetic field. The only effect of the magnetic field is that the electron mass is effectively incremented by a B-dependent factor, and the tunneling exponent $R\equiv R_1$ is appropriately renormalized: $m\rightarrow m^*$ and $R\rightarrow(m^*/m)^{1/2}R_{B=0}$, with

$$m^*\approx m\left[1+\frac{\omega_c^2}{2m}\int_0^{\tau_f}d\tau\,\tau^2\chi(\tau)\right]$$

$$\approx m\left[1+(2N)^{-1}\sum_{\mathbf{k}j}(\omega_c^2/\omega_{\mathbf{k}j}^2)\right]. \quad (11)$$

Here, we assume that the major contribution to the integral over τ comes from times $\tau\sim1/\omega_p\ll\tau_f$. Respectively, for a Wigner crystal, the major contribution to the sum over $(\mathbf{k},j)$, comes from $\omega_{\mathbf{k}j}\sim\omega_p$. The integral only weakly depends on the upper limit τ_f, which also provides the inverse of the lower cutoff frequency in the sum over $(\mathbf{k},j)$. For a Wigner crystal, the dependence of the mass renormalization on τ_f is logarithmic.

The tunneling rate approaches its value for $B=0$ with increasing ω_p. On the other hand, the slope of the logarithm of the tunneling rate as a function of ω_c depends explicitly on ω_p. This provides a means for measuring ω_p.

For $\omega_p\tau_f\sim1$, only a part of the Hall momentum can be taken by the electron crystal. The rest goes into the in-plane kinetic energy of the tunneling electron, and ultimately into creations of WC phonons. However, the tunneling exponent R_n usually *decreases* with increasing phonon frequencies. This is because the more rigid the electron system is, the more effectively it compensates the in-plane Hall momentum.

The relative role of phonons of different frequencies and wave numbers can be characterized by the density of states weighted with the interaction $J(\omega)$, see Ref. 21. From Eq. (8), for the coupling H_B

$$J(\omega)=(m/\gamma_1^2N)\sum_{\mathbf{k}j}\omega_{\mathbf{k}j}\,\delta(\omega-\omega_{\mathbf{k}j}).$$

The small-ω behavior of $J(\omega)$ is determined primarily by transverse acoustic phonons, with $J(\omega)\propto\omega^2$. This corresponds to "superohmic" dissipation, according to the nomenclature.[21] The effect on tunneling of low-frequency phonons is comparatively small in this case, which is not surprising, because the coupling is *kinematic*, the tunneling electron is coupled to the phonon momenta $\mathbf{p}_{\mathbf{k}j}$. The major effect on R_n comes from high-frequency short-wavelength phonons, which have large density of states. An important consequence is that tunneling is influenced primarily by short-range order in the electron system.

On the whole, for $T=0$, the magnetic-field induced term in the tunneling exponent is positive, i.e. the tunneling rate decreases with the magnetic field. This can be seen from Eqs. (6), (7) by replacing $z(\tau_1)z(\tau_2)$ in $\mathcal{R}_{ee}$ with $(1/2)[z^2(\tau_1)+z^2(\tau_2)]\geq z(\tau_1)z(\tau_2)$ and then integrating the function $\chi(\tau_1-\tau_2)$ over τ_2 [for the term $z^2(\tau_1)$] or τ_1 [for $z^2(\tau_2)$]. For specific models, the dependence of the tunneling rate on B and the vibration frequencies will be illustrated in Sec. V, and the results will be compared with the experiment.

C. High temperatures and small phonon frequencies

The analysis of the tunneling rate somewhat simplifies in the case of comparatively high temperatures and small phonon frequencies, where the vibrations are classical and their frequencies are small compared to the reciprocal tunneling duration $\omega_{\mathbf{k}j}\beta,\omega_{\mathbf{k}j}\tau_f\ll1$. In this case

$$\mathcal{R}_{ee}[z]=-2mT\omega_c^2\tau_f^2\bar{z}^2,\quad \bar{z}=\tau_f^{-1}\int_0^{\tau_f}d\tau\,z(\tau).\quad(12)$$

Equations (6), (12) also describe the tunneling action of a single electron, with the Maxwell distribution of the in-plane momentum inside the well $\exp(-p^2/2mT)$. The coupling of the $\hat{\mathbf{z}}\times\mathbf{B}$ component of the momentum to the out-of-plane motion gives rise to the term $-2p\omega_c\int_0^{\tau_f}d\tau\,z(\tau)$ in the tunneling action [see Eqs. (4), (A3)]. The extreme value of the sum of this term and $-p^2/2mT$ is just equal to $-\mathcal{R}_{ee}[z]$ as given by Eq. (12).

The single-electron form of the tunneling exponent is to be expected in the limit of small $\omega_{\mathbf{k}j}$, because the distribution over in-plane momenta of electrons forming a Wigner crystal is Maxwellian, in the classical limit. For small $\omega_{\mathbf{k}j}\tau_f$ the momenta do not change over the tunneling duration, therefore only the momentum of the tunneling electron itself is important. The above derivation provides an independent test of the derivation used to obtain the general expressions (6), (7).

We note that the action $\mathcal{R}_{ee}[z]$ (12) is still retarded, it does not correspond to a local in time Lagrangian. The func-

tional form of $\mathcal{R}_{ee}$ remains the same even for temperatures $T \lesssim \omega_{\mathbf{k}j}$ provided the phonon frequencies are small compared to τ_f^{-1} and ω_c. In this case T in Eq. (12) has to be replaced by $(4N)^{-1} \Sigma \omega_{\mathbf{k}j}(2\bar{n}_{\mathbf{k}j}+1) \equiv \chi(0)/2m$. This factor explicitly depends on the phonon dispersion law, but again, the major contribution comes from short-wavelength high-frequency phonons, which are determined by the short-range order in the electron system.

IV. ENHANCEMENT OF TUNNELING BY A MAGNETIC FIELD

In this section we show that a parallel magnetic field can enhance the rate of tunneling from the electron layer. Qualitatively, the enhancement is due to transferring the energy of thermal in-plane motion into the energy of out-of-plane tunneling. On the formal level it is a consequence of the increase, with increasing temperature, of the absolute value of the term $\mathcal{R}_{ee}$ (7) in the tunneling action. Since this term gives a negative contribution to the tunneling exponent, the whole B-dependent term in $\mathcal{R}$ becomes negative starting with a certain crossover temperature T_{cr}, and then the tunneling rate increases with B. The region where the overall escape rate increases with B is not universal and depends on the potential $U(z)$ and the phonon spectrum. The enhancement occurs in a limited temperature range, and may start from $B=0$ or have a finite threshold in B. However, very strong fields suppress rather than enhance escape.

A. Small magnetic fields: The crossover temperature

The lower temperature bound of the enhancement domain is the crossover temperature T_{cr}. It can be determined from the small-B expansion of the tunneling exponent for the ground state $n=1$ in Eq. (5) (we use the subscript g for this state),

$$R_g(B) \approx R_g(0) + A_g(T)\omega_c^2, \quad \omega_c \tau_0 \ll 1, \quad (13)$$

where τ_0 is the tunneling time in the ground state (with energy $E=E_g$) for $B=0$. The role of the ground state is special in that the barrier width here is usually bigger than for the excited states. Therefore the effect of the magnetic field, which accumulates under the barrier, is most pronounced in the ground state.

The value of A_g is given by the terms $\propto \omega_c^2$ in the action R_g (6) calculated along the tunneling trajectory $z_0(\tau)$ for $B=0$. From the analysis in Sec. III B it follows that $A_g>0$ for $T \to 0$. The crossover temperature is given by

$$A_g(T_{cr}) = 0. \quad (14)$$

For $T > T_{cr}$ the tunneling exponent R_g decreases and the tunneling rate increases with B, in the region of comparatively small B.

In the limit of low phonon frequencies, $\omega_{\mathbf{k}j} \ll 1/\tau_0, T_{cr}$, from Eqs. (6), (12) it follows that $\beta_{cr} \equiv 1/T_{cr} = 2\tau_0 \bar{z}_0^2/\overline{z_0^2}$, where $\bar{z}_0$ is the average coordinate $\bar{z}$ (12) for the $B=0$ trajectory with energy E_g, and $\overline{z_0^2}$ is the mean square value of z on the same trajectory

$$\overline{z_0^2} = \tau_0^{-1} \int_0^{\tau_0} d\tau\, z_0^2(\tau) \quad (E=E_g).$$

One can see that $\beta_{cr} < 2\tau_0$. It follows from Eq. (7) that $2\tau_0$ is also the limiting value of β_{cr} in the opposite case of high phonon frequencies $\omega_{\mathbf{k}j} \gg 1/\tau_0$. On the whole, we have the following bounds on temperature for the tunneling enhancement in the ground intrawell state:

$$2\tau_0 \frac{\bar{z}_0^2}{\overline{z_0^2}} < \beta_{cr} < 2\tau_0. \quad (15)$$

Generally $\bar{z}_0^2/\overline{z_0^2} \sim 1$.

It follows from the above arguments that the value of the crossover temperature $T_{cr} = 1/\beta_{cr}$ decreases with increasing phonon frequencies, that is the crossover is determined by high-frequency phonons which, in the case of 2D electron systems, have large wave numbers and are determined by the short-range order. We emphasize that there is no threshold in B for tunneling enhancement in the range (15) provided the system tunnels from the ground state.

B. Small magnetic fields: Upper temperature limit for enhancement

The tunneling rate may increase with B in the excited states, too. However, this does not happen for simple model potentials investigated below. If the tunneling is enhanced only in the ground state, the upper temperature bound of the enhancement domain is often the temperature $T_{1 \to 2}$ where the probability of tunneling from the first excited state, weighted with the occupation factor, exceeds that from the ground state, for $B=0$. It can be estimated for smooth tunneling barriers where, for $B=0$, the tunneling duration as a function of energy $\tau_0(E)$ decreases with the increasing energy E, which is often the case. From Eq. (6), switching between tunneling from the ground ($n=1$) and first excited state ($n=2$) occurs for the reciprocal temperature

$$\beta_{1 \to 2} = 2\frac{\int_{E_1}^{E_2} \tau_0(E)dE}{E_2 - E_1} \quad (E_1 \equiv E_g).$$

This value lies between $2\tau_0(E_2)$ and $2\tau_0(E_1)$. Depending on the tunneling potential, $\beta_{1 \to 2}$ can be smaller or larger than β_{cr} (15). If a magnetic field does not increase the rate of tunneling from the state $n=2$, the field-induced tunneling enhancement starting with $B=0$ occurs for $T_{cr} < T < T_{1 \to 2}$.

C. Field-induced switching between the levels and from activation to tunneling

Even in the temperature range $T > T_{1 \to 2}$ a sufficiently strong magnetic field can increase the tunneling rate, provided $T > T_{cr}$. This happens if the tunneling exponent for the ground state $R_g(0) \equiv R_{n=1}(0)$ exceeds $R_{n=2}(0)$. Then within a certain temperature range the escape rate for $B=0$ is determined by tunneling from the excited state $n=2$. The rate of this tunneling decreases with increasing B ($R_{n=2}$ in-

creases with B). For some B the exponents $R_{n=2}(B)$ $+\beta(E_2-E_1)$ and $R_{n=1}(B)$ become equal to each other. For larger B the system tunnels from the ground state, and the tunneling rate increases with B.

Similarly, since the activation rate is often weakly affected by B, in a certain temperature range where escape already occurs via activation for $B=0$, starting with some B it may again go through tunneling from the ground state. This happens if the tunneling rate for the ground state becomes bigger than the activation rate, and can be observed only in a limited range of B, as discussed in Sec. V for T_{cr} $<T_{1\rightarrow 2},T_a$. For a special model the switching is illustrated in Fig. 5 below. We note that, in principle, the B-induced enhancement of the escape rate may occur in a limited B range even for $T_{cr}>T_{1\rightarrow 2},T_a$ (we assume here that thermalization inside the well occurs before the electron escapes).

V. TUNNELING ENHANCEMENT FOR THE EINSTEIN MODEL OF A WIGNER CRYSTAL

In what follows we will illustrate the general results and apply them to specific 2D systems assuming that all vibrational modes have the same frequency, $\omega_{kj}=\omega_p$, i.e., using the Einstein model of the Wigner crystal. This is motivated by the results of Sec. III B that the tunneling is determined primarily by short-wavelength vibrations, which have a comparatively weak dispersion. When discussing the experiment, we will set ω_p equal to the characteristic short-wavelength plasma frequency $(2\pi e^2 n^{3/2}/m)^{1/2}$, where n is the electron density.

A. Triangular barrier

For electrons above helium surface and in certain types of semiconductor heterostructures, the potential $U(z)$ in the barrier region is largely determined by the electric field which pulls electrons away from the intrawell states. To a good approximation $U(z)$ is then linear in z for $z\geq z_{in}$, and if we set $z_{in}=0$, we have

$$U(z)=\frac{\gamma^2}{2m}\left(1-\frac{z}{L}\right)\quad(z\geq 0). \tag{16}$$

Here, $\gamma\equiv\gamma_1$ is the decrement of the ground-state wave function $\psi_g\equiv\psi_1$ near the well, $\partial\ln\psi_1/\partial z=-\gamma$ for $z=0$, see the discussion before Eq. (9). The additive constant in $U(z)$ is chosen so that the energy of the ground state $E_g=0$. Then L is the tunneling length in the ground state for $B=0$. It is determined by the pulling electric field. We assume that $\gamma L\gg 1$.

The approximation (16) applies only within the barrier region, and not inside the well, where $U(z)$ is singular. Moreover, it holds provided the width of the tunneling barrier is small compared to the in-plane interelectron distance $n^{-1/2}$ [see Eq. (24) below].

In order to calculate the ground-state tunneling exponent, it is convenient to solve directly the equations of motion of the electron and phonons under the barrier (A6) with the

boundary conditions (9), (10), (A12), and (A14). For a triangular potential, these equations are linear. This allowed us to obtain a simple expression for the tunneling exponent

$$\tilde{R}=-\nu_p^2\tau_{red}^3+3\nu_p\tau_{red}(1-\tau_{red})\coth[\omega_p\beta/2-\nu_p\tau_{red}]$$
$$+3+3\tau_{red}(\nu^2-1),\quad R_g=2\gamma L\tilde{R}/3\nu^2. \tag{17}$$

Here, $\nu_p=\omega_p\tau_0$ and $\nu_c=\omega_c\tau_0$ are, respectively, the dimensionless in-plane and cyclotron frequencies scaled by the tunneling duration τ_0 for $B=0$, and $\nu^2=\nu_p^2+\nu_c^2$.

The quantity $\tau_{red}=\tau_f/\tau_0$ in Eq. (17) is the reduced tunneling duration. It is given by the equation

$$[(1-\tau_{red})\nu_p\nu^2\coth[\omega_p\beta/2-\nu_p\tau_{red}]-\nu_c^2]\tanh\nu\tau_{red}$$
$$=\nu[\nu_p^2\tau_{red}-\nu^2]. \tag{18}$$

In the limit $T\rightarrow 0$, Eqs. (17), (18) go over into the result obtained earlier[6] (in Ref. 6 we used ω_0 and ν_0 instead of ω_p and ν_p). In this limit, the role of the many-electron effects is particularly important. In the single-electron approximation ($\omega_p=0$) the tunneling duration τ_f and the tunneling exponent R_g diverge for $\omega_c\rightarrow\tau_0^{-1}$.[5] This happens because the effective single-electron potential $U(z)+(1/2)m\omega_c^2z^2$, which takes into account the parabolic magnetic barrier, does not have classically allowed extended states with energy $E_g=0$ behind the barrier.

The interelectron momentum exchange makes tunneling possible for all B. For $\omega_c\tau_0>1$ and $T=0$, the tunneling exponent is a steep function of the exchange rate ω_p in the limit of slow exchange, $\omega_p\tau_0\ll 1$. In the opposite limit of the fast momentum exchange, $\omega_p\gg\tau_0^{-1},\omega_c$, from Eqs. (17), (18) we obtain $\tau_{red}\approx 1$ [i.e., $\tau_f\approx\tau_0$], and $R_g\approx 4\gamma L/3$. These are the values for tunneling for $B=0$. The overall dependence of the tunneling exponent on ω_p for $T=0$ is shown in the inset of Fig. 3.

For a given magnetic field, the dependence of the tunneling exponent R_g on the frequency ω_p becomes less steep with increasing temperature, as seen from Fig. 3. This is because thermal in-plane motion of the tunneling electron becomes more important than interelectron momentum exchange with increasing temperature. For large $\omega_p\tau_0,\omega_p\beta$, the curves for different temperatures merge together and approach the $B=0$ asymptote.

The value of R_g can be calculated independently from the functional $\mathcal{R}_n$ (6) using the direct variational method. Even a simple approximation where $z(\tau)$ is quadratic in τ, with the only variational parameter being the tunneling duration τ_f, gives a reasonably good result. For the highest temperature in Fig. 3, it is shown by the dashed line. Such calculation gives a good approximation for higher temperatures, and also for lower temperatures but not too small $\omega_p\tau_0$. For low tem-
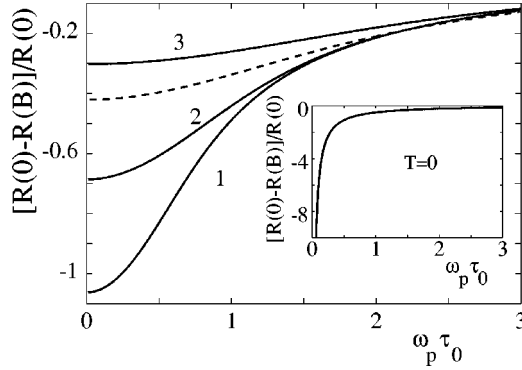
FIG. 3. The tunneling exponent in the ground state $R(B)$ $\equiv R_g(B)$ for a triangular potential barrier (16) as a function of the phonon frequency ω_p in the Einstein model of the Wigner crystal for $\omega_c \tau_0 = 2$. The time $\tau_0 = 2mL/\gamma$ is the duration of tunneling for $B = 0$ and $T = 0$. The curves 1 to 3 refer to reciprocal temperatures $\beta/\tau_0 = 7$, 5, 3. The dashed line is the result of the direct variational method for $\beta = 3\tau_0$, with one variational parameter τ_f.

peratures and small $\omega_p \tau_0$ the trajectory $z(\tau)$ is strongly non-parabolic, and more than one parameter is required in the variational calculation.

B. Field-induced tunneling enhancement and switching to tunneling from activation

The explicit expression for the tunneling exponent (17) allows us to analyze the tunneling enhancement and the magnetic field induced switching to tunneling discussed in Sec. IV. In the small-B limit, where $\omega_c \ll \omega_p, \tau_0^{-1}$, the tunneling exponent $R_g(B)$ is seen from Eq. (17) to be quadratic in B. The coefficient A_g in Eq. (13) can be easily calculated. From the condition $A_g = 0$ we obtain the value of the reciprocal temperature β_{cr} which corresponds to the crossover from decrease to increase of the tunneling rate due to a magnetic field

$$\beta_{cr} = 2\tau_0 + \frac{2}{\omega_p} \tanh^{-1} \left[\frac{\nu_p [3\nu_p - (3 + \nu_p^2) \tanh \nu_p]}{\nu_p^3 - 3\nu_p + 3\tanh \nu_p} \right].$$

(19)

In agreement with (15), β_{cr} monotonically increases with ω_p from $5\tau_0/3$ at $\omega_p = 0$ to $2\tau_0$ for $\omega_p \to \infty$.

The dependence of the tunneling exponent (17) on the magnetic field for different temperatures is shown in Fig. 4. Above the crossover temperature ($\beta < \beta_{cr}$), $R_g(B)$ *decreases* with B. Then $R_g(0) - R_g(B)$ and the tunneling probability *increase* with the increasing field, for small B. The slope $dR_g/dB^2 \propto \beta - \beta_{cr}$ for $B \to 0$. However, for strong fields the tunneling rate decreases with the increasing B, because the Hall momentum can no longer be compensated by thermal fluctuations.

It is clear from the data in Fig. 4 that, for the barrier chosen, the magnetic field induced increase of the tunneling exponent R is numerically small. However, for typical $R \gtrsim 50$ it can still be noticeable.

The expression (17) gives the tunneling exponent only for low enough temperatures where the system escapes from the
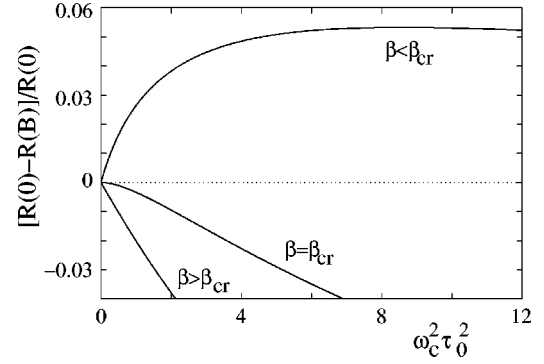

FIG. 4. The dependence of the tunneling exponent $R(B)$ $\equiv R_g(B)$ on the magnetic field (17) for $\omega_p \tau_0 = 1/3$ near the crossover temperature $\beta_{cr} \approx 1.67\tau_0$ (19). The curves 1 to 3 correspond to $(\beta - \beta_{cr})/\tau_0 = 0.2, 0, -0.3$.

ground state. For higher temperatures, one should take into account the possibility of escape from excited states and via an activated transition over a potential barrier. The positions of the excited levels depend not only on the barrier shape, but also on the shape of the potential $U(z)$ inside the well. The analysis for a specific system, electrons on the surface of liquid helium, is done in the next section. Here, in order to illustrate different scenarios, we discuss two cases: a narrow well, in which case the ground state is essentially the only intrawell state, and a well with a comparatively shallow excited state. We assume that the intrawell relaxation rate is higher than the escape rate.

We start with the case of one bound state in the potential well. Here, for $B = 0$ switching from tunneling to activation occurs for the temperature $T_a \equiv 1/\beta_a = (4\tau_0/3)^{-1}$. This temperature is higher than the crossover temperature $1/\beta_{cr}$ (19), and therefore there is a region where the enhancement of tunneling by a magnetic field can be observed, as discussed above (see Fig. 4). However, even though for $T > T_a$ the B
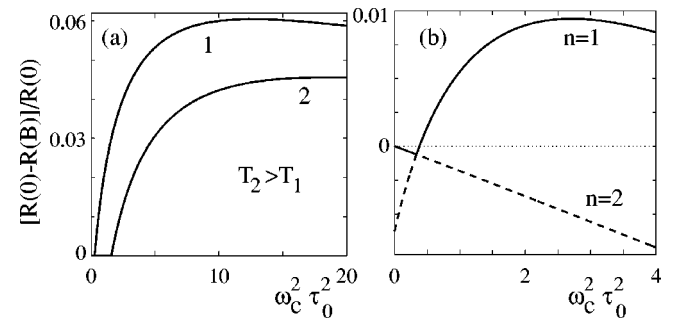

FIG. 5. Magnetic field induced switching from activation (a) and from tunneling from the excited state (b) to tunneling from the ground state, for $\omega_p \tau_0 = 1/3$ (respectively, $\beta_{cr} \approx 1.67\tau_0$). The escape exponent $R = \min_n [R_n + \beta(E_n - E_1)] \propto -\ln W$. In (a), there is only one intrawell state in the potential well $U(z)$, and the transition to activation for $B = 0$ occurs for $\beta/\tau_0 = 4/3$. The curves 1, 2 correspond to $(\beta - \beta_{cr})/\tau_0 = -0.35, -0.4$. In (b), the position E_2 of the excited level ($n = 2$) is chosen at $0.2\gamma^2/2m$ below the barrier top. The temperature is chosen at $(\beta - \beta_{cr})/\tau_0 = -0.16$, so that for $B = 0$ the system tunnels from the excited state. The observable (smaller) exponent $R_n + \beta E_n$ for a given B is shown with the bold line, whereas the dashed line shows the bigger exponent.

$=0$ escape occurs via overbarrier transitions, the increase of the tunneling rate with the increasing B can make tunneling more probable for sufficiently strong B. If the activation rate is independent of B, the overall dependence of the exponent of the escape rate $R(B) = \min_n[R_n(B) + \beta(E_n - E_1)]$ $\propto -\ln W(B)$ on B is shown in Fig. 5(a). In this case, $R(0) = \gamma^2/2mT$ is the barrier height over temperature. Switching to tunneling and the increase of the escape rate with B occur where the tunneling exponent $R_g(B)$ as given by Eq. (17) becomes less than $R(0)$.

Similar switching occurs in the temperature range where tunneling from the first excited level is more probable than from the ground state, for $B = 0$. With increasing B, the tunneling rate in the excited state decreases, whereas in the ground state it increases, and therefore starting with certain B, the system switches to tunneling from the ground state. This is illustrated in Fig. 5(b).

C. Square barrier: Field-induced crossover to thermal activation

In many physically interesting systems, the tunneling barrier $U(z)$ is nearly rectangular. This is often the case for semiconductor heterostructures, where the barrier is formed by the insulating layer. If we count U off from the intrawell energy level E_g and set the boundaries at $z = 0$ and $z = L$, the barrier has the form

$$U(z) = \gamma^2/2m, \quad 0 < z < L. \tag{20}$$

Here, $1/\gamma$ is the decay length under the barrier, see Eq. (9), and we have neglected the lowering of the barrier due to the electrostatic field from other electrons at their lattice sites, which is a good approximation for the interelectron distance $n^{-1/2} \ll L$.

We assume that, behind the barrier $(z > L)$, an electron can move semiclassically with all energies. Then the decaying underbarrier wave function has to be matched to an appropriate propagating wave behind the barrier at $z = L$. In contrast to the case of a smooth barrier, because the potential $U(z)$ is discontinuous at $z = L$, the z component of the momentum should not be the same on the opposite sides of the boundary. However, the in-plane "momentum" compo-

nents of the phonons $\mathbf{u}_{kj}$, which are imaginary under the barrier, still have to be continuous. Respectively, the boundary conditions (A7) for the tunneling trajectory should be changed to

$$z(\tau_f) = L, \quad \mathbf{u}_{kj}(\tau_f) = \mathbf{0} \tag{21}$$

(τ_f is the imaginary time at which the boundary is reached).

With the boundary conditions (21), elimination of phonon variables from the Euclidean action in the tunneling exponent is similar to what was done for a smooth barrier in the Appendix. The resulting expression for the retarded action functional $\mathcal{R}_n[z]$ coincides with Eq. (6), provided $z(\tau_f + \tau)$ is *defined* as $z(\tau_f - \tau)$, for $0 \leq \tau \leq \tau_f$.

An important feature of a rectangular tunneling barrier is that, for $B = 0$, the tunneling time $\tau_0(E) = -(1/2)dR_n/dE_n$ monotonically increases with energy E_n. Therefore the maximum of the function $-\beta E - R(E)$, which gives the escape probability, corresponds either to the transition from the ground state or to activation over the barrier. Switching to activation occurs for the temperature $T_a = \gamma^2/2mR_g(0) \equiv \gamma/4mL = (4\tau_0)^{-1}$. It is less than 1/2 of the temperature T_{cr} of the crossover from B-suppressed to B-enhanced tunneling as given by Eq. (15), and therefore we do not expect the crossover to occur in systems with a square barrier.

For temperatures $T < T_a$ and $B = 0$, escape occurs via tunneling, and its probability decreases with the increasing B. Starting with some B, where the tunneling exponent becomes bigger than the activation exponent $\gamma^2/2mT$, it becomes more probable to escape via an activated transition. Then the magnetic field dependence of the escape rate becomes much weaker.

The B dependence of the escape rate for different temperatures is illustrated in Fig. 6. The results refer to the Einstein model of the Wigner crystal. In this model the tunneling exponent can be obtained directly from the [linear, in this case] equations of motion (A6) with the boundary conditions (9), (A12), (21). It has the form

$$R_g = \gamma L[1 + \tau_{red} + \nu_c \kappa(\tau_{red})], \tag{22}$$

where the function $\kappa(\tau_{red})$ and the reduced tunneling time $\tau_{red} = \tau_f/\tau_0$ are given by the equations

$$\kappa(\tau_{red}) \equiv \frac{\nu_c(\cosh \nu\tau_{red} - 1)}{\nu_c^2 + \nu_p^2\cosh \nu\tau_{red} + \nu\nu_p\coth[\omega_p\beta/2 - \nu_p\tau_{red}]\sinh \nu\tau_{red}}$$

$$= \frac{1}{\nu_c\nu_p^2} \frac{\nu_c^2(2 - 2\cosh \nu\tau_{red} + \nu\tau_{red}\sinh \nu\tau_{red}) - \nu^3(\tau_{red} - 1)\sinh \nu\tau_{red}}{(1 - \cosh \nu\tau_{red})(1 - \nu_c^2/\nu_p^2) + \nu\tau_{red}\sinh \nu\tau_{red}} \tag{23}$$

with $\nu_p = \omega_p\tau_0$, $\nu_c = \omega_c\tau_0$, and $\nu = (\nu_p^2 + \nu_c^2)^{1/2}$.

The temperature of switching to activation is given by the equation $T_a = \gamma^2/2mR_g$. From Eqs. (22), (23), R_g increases with the magnetic field. Therefore the switching temperature

T_a does not exceed $1/4\tau_0 = \gamma^2/2mR_g(B=0)$ and decreases with B.

The effect of saturation of the escape rate with increasing B shown in Fig. 6 is not limited to square barriers, of course.

For strong enough B and nonzero temperatures, the tunneling rate becomes smaller than the activation rate, and the system switches to activation; the switching may go in steps with increasing B, via tunneling from excited intrawell states.

VI. COMPARISON WITH THE EXPERIMENTAL DATA ON TUNNELING FROM HELIUM SURFACE

Tunneling from a strongly correlated 2DES has been investigated in much detail for electrons on helium surface.[22,5] In this system, a good agreement has been reached between theory and experiment in the absence of the magnetic field, where the primary role of the electron correlations is to change the effective single-electron tunneling barrier (see below). As mentioned before, there were also done interesting experiments on tunneling in a magnetic field. However, the observed strong field dependence of the tunneling rate dramatically differed from the predictions of the single-electron theory and remained unexplained[5] (the data for the lowest temperature have been compared to the theory for $T=0$ in Ref. 7).

Electrons on helium surface are localized in a 1D potential box. The smooth side of this box is the image potential $-\Lambda/z$, where $\Lambda=e^2(\epsilon-1)/4(\epsilon+1)$ ($\epsilon\approx1.057$ is the dielectric constant of helium), and z is the direction normal to the surface. The other side is a steep high barrier ~1 eV on the surface ($z=0$), which prevents electrons from penetrating into the helium. The intrawell states can be made metastable by applying a field $\mathcal{E}_\perp$ which pulls the electrons away from the surface. This field is determined by the helium cell geometry and depends on the applied voltage and the electron density n, see Ref. 23. The overall electron potential has the form

$$U(z)=-\Lambda z^{-1}-|e\mathcal{E}_\perp|z-m\bar{\omega}^2z^2 \quad (z>0). \tag{24}$$
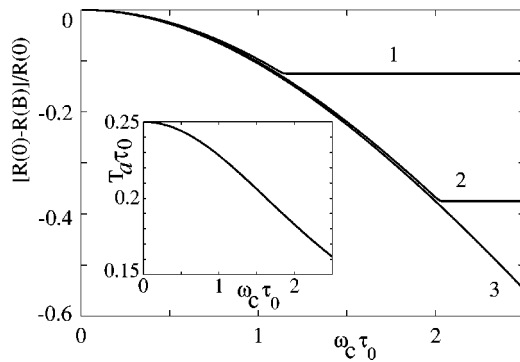

FIG. 6. The logarithm of the escape rate $R(B)$ $=\min[R_g,\gamma^2/2mT]$ for the square potential barrier and for ω_p $=(2\tau_0)^{-1}$ ($\tau_0=mL/\gamma$). The value $R(0)$ is given by the tunneling exponent $R(0)=2\gamma L$. Curves 1 to 3 correspond to β/τ_0 $=4.5,5.5,6.5$. The sections of the curves where $R(B)$ increases correspond to tunneling and are described by Eq. (22), whereas the horizontal sections of the curves correspond to thermal activation. Inset: the magnetic field dependence of the switching temperature $T_a\tau_0$.
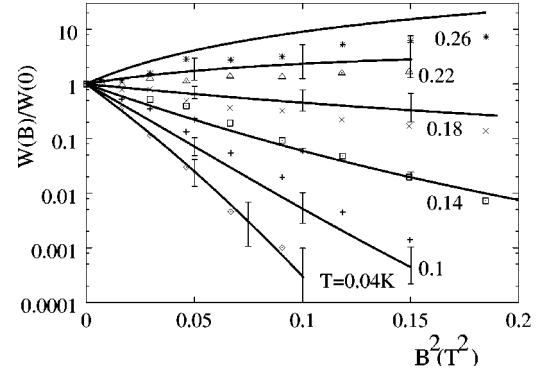

FIG. 7. The relative rate of electron tunneling from the helium surface $W(B)/W(0)$ as a function of the magnetic field B for the electron density $n=0.8\times10^8$ cm^{-2} and the calculated pulling field $\mathcal{E}_\perp=24.7$ V/cm. Solid lines show how the theory compares to the experimental data points of Ref. 5. The error bars show the uncertainty in the theoretical values due to the uncertainty in the parameters of the experiment.

The term $\propto\bar{\omega}^2$ describes the Coulomb field created by other electrons at their in-plane lattice sites (the "correlation hole"[17,24]). Only the lowest-order term in the ratio of the tunneling length L to the interelectron distance $n^{-1/2}$ has been kept in Eq. (24), and

$$\bar{\omega}=\left[\frac{e^2}{2m}\sum_l{}'\,|\mathbf{R}_l|^{-3}\right]^{1/2}\equiv\left[\frac{1}{2N}\sum_{\mathbf{k}j}\omega_{\mathbf{k}j}^2\right]^{1/2} \tag{25}$$

is given by the sum over lattice sites $\mathbf{R}_l$. For a triangular lattice, $\bar{\omega}\approx(4.45e^2n^{3/2}/m)^{1/2}$.[25] The conditions $1/\gamma\ll L$ $\ll n^{-1/2}$ are typically very well satisfied in experiment, with the decay length $1/\gamma=1/\Lambda m\approx0.7\times10^{-6}$ cm, $L\sim|E_g/e\mathcal{E}_\perp|$ $\approx\gamma^2/2m|e\mathcal{E}_\perp|\sim10^{-5}$ cm, and $n^{-1/2}\sim10^{-4}$ cm (in the estimate of L we used that $|E_g|\gg|e\mathcal{E}_\perp|/\gamma$, $m\bar{\omega}^2/\gamma^2$, and that $|e\mathcal{E}_\perp|/\gamma\gtrsim\bar{\omega}$).

To compare the predicted dynamical effect of the electron-electron interaction with the experimental data on tunneling in the magnetic field,[5] we use the Einstein model of the WC and set all phonon frequencies $\omega_{\mathbf{k}j}$ equal to the characteristic plasma frequency $\omega_p=(2\pi e^2n^{3/2}/m)^{1/2}$. The numerical results change only slightly when the phonon frequency is varied within reasonable limits, e.g., is replaced by $\bar{\omega}$; in the expression for $U(z)$ we use $\bar{\omega}$ as given by Eq. (25).

The calculated magnetic field dependence of the tunneling rate for the parameters used in the experiment is shown in Fig. 7. The data refer to the values of T where escape occurs via tunneling from the ground state. The actual calculation is largely simplified by the fact that, deep under the barrier, the image potential $-\Lambda/z$ in Eq. (24) can be neglected. The equations of motion (A6) become then linear, and the tunneling exponent R_g can be obtained in an explicit, although cumbersome form, which was used in Fig. 7. The correction to R_g from the image potential is $\sim1/\gamma L$, which is the small parameter of the theory. Moreover, since this correction comes from the range of small z, where the effect of the magnetic field is small, it is largely compensated where $R_g(B)-R_g(0)$ is calculated. This and other corrections

$\sim 1/\gamma L$ result in changes of the theoretical curves that are smaller than the uncertainty in $R_g(B) - R_g(0)$ due to the uncertainties in n and $\mathcal{E}_\perp$ in the experiment.[5]

As seen from Fig. 7, the dynamical many-electron theory is in good qualitative and quantitative agreement with the experiment, without any adjustable parameters. At low temperatures ($T = 0.04$ K), the many-electron tunneling rate is bigger than the single-electron estimate[5] by a factor of 10^2 for $B = 0.25$ T. For this temperature, the tunneling rate is well described by the $T \to 0$ limit.[7] The B dependence of the tunneling rate is very sensitive to temperature. The role of dynamical many-electron effects becomes less important for higher T. Interestingly, the theoretical data on the *ratio* of $W(B)/W(0)$ become less sensitive to the experimental uncertainties in the cell geometry (which determines $\mathcal{E}_\perp$) and the electron density n for intermediate temperatures $T \sim 0.14$ K. This is because the corresponding errors in $W(B)$ and $W(0)$ compensate each other for such temperatures.

The crossover to magnetic-field enhanced tunneling occurs for temperature $T_{cr} \approx 0.19$ K, for the parameters in Fig. 7. The expected increase of the tunneling rate with B for $T > T_{cr}$ is shown in Fig. 7. It has indeed been observed in the experiment.[5] The analysis of the experiment requires to establish whether, for temperatures of interest, escape actually occurs via tunneling. To that end we note first that, as it follows from a direct variational calculation, the potential $U(z)$ (24), with the parameter values specified in Fig. 7, has only one metastable intrawell state. Electrons are initially prepared in this state.

If the intrawell relaxation were fast enough, the temperature of the crossover from tunneling to activation T_a for $B = 0$ would be given by the condition that the tunneling exponent R_g be equal to the activation exponent $(U_{max} - E_g)/T$ [here, U_{max} is the maximal value of the potential $U(z)$]. This would give $T_a \approx 0.15$ K. However, activated escape requires that the in-plane thermal energy of an electron be transformed into the energy of its out-of-plane motion. This involves a large transfer of the in-plane momentum $\sim [2m(U_{max} - E_g)]^{1/2}$. The electron-electron interaction does not give rise to such a transfer in a strongly correlated system, since the reciprocal interelectron distance is $n^{1/2} \ll [2m(U_{max} - E_g)]^{1/2}$.

The major momentum transfer mechanism is scattering by capillary waves on the helium surface, ripplons.[2] Electron-ripplon coupling is weak. As a result, the prefactor in the activation rate, which is quadratic in the coupling constant, is small. For $B = 0$ it is $\sim \gamma^2 T^2/\hbar\sigma$,[26] where σ is the surface tension of liquid helium, and for $T < 0.25$ K it is smaller than the prefactor in the tunneling rate $(\hbar\gamma^2/m)\exp(-2)$ by a factor $< 10^{-5}$. Therefore the crossover from tunneling to activation occurs for higher temperatures than it would follow from the condition of equal tunneling and activation exponents.

For the parameters in Fig. 7, the rates of activation and tunneling escape become equal for temperatures slightly higher than 0.26 K (for $B = 0$). Therefore we believe that the experimentally observed increase of the escape rate with B is due to the discussed mechanism of B-enhanced tunneling.

The smaller experimental values of the relative escape rate $W(B)/W(0)$ for $T = 0.26$ K can be understood by noticing that the activation rate is close to the tunneling rate for such T, and since it presumably only weakly depends on B,[27] the overall slope of $\ln[W(B)/W(0)]$ should be smaller than that of the theoretical curve which ignores activation (by a factor ~ 2, according to an estimate which ignores the dependence of the activation rate on B). Therefore we do not show error bars for this curve.

The prefactor

The dependence of the potential $U(z)$ (24) on n gives rise to the density dependence of the tunneling rate even for $B = 0$. We calculated the exponent and the prefactor in $W = W(B = 0)$ by matching the WKB wave function under the barrier for $1/\gamma \ll z \ll L$ with the tail of the non-WKB intrawell solution (here, $L = \hbar^2\gamma^2/2m|e\mathcal{E}_\perp|$ is the characteristic barrier width). In the spirit of the logarithmic perturbation theory (LPT),[28] the wave function of the ground state inside the well and not too far from it can be sought in the form

$$\psi_g(z) = \text{const} \times z \exp[-A(z)] \qquad (26)$$

[we take into account that the function $\psi_g(z)$ has one zero, which is located at the helium surface, $z = 0$].

The function dA/dz satisfies a Riccati equation. It can be solved near the well ($z \ll L$) by considering the last two terms in the potential $U(z)$ (24) as a perturbation. For small z, the major correction comes from the term $\propto \mathcal{E}_\perp$. To the first order in $\mathcal{E}_\perp$,

$$A(z) \approx \gamma z \left(1 - \frac{z}{4L}\right). \qquad (27)$$

In obtaining this expression we took into account the correction to the ground state energy $\delta E_g = -3|e\mathcal{E}_\perp|/2\gamma$. This correction can be obtained from the condition that the linear in $\mathcal{E}_\perp$ term in dA/dz remain finite for $z \to 0$.

The correction to A (27) is small for z small compared to the barrier width L. We note that the exponent $A(z)$ has an overall functional form which differs from that of the commonly used[2] variational wave function $\psi(z) \propto z \exp(-\tilde{\gamma}z)$, with $\tilde{\gamma}$ being a variational parameter.

The expression for A (27) matches the small-z/L expansion of the action S of the WKB wave function under the barrier for $L \gg z \gg \gamma^{-1}$. This allowed us to find the prefactor in the WKB wave function and in the tunneling rate. The resulting tunneling rate is shown in Fig. 8. It fully agrees with the experiment (see also Ref. 22).

VII. CONCLUSIONS

It follows from the results of the present paper that tunneling in a magnetic field parallel to the electron layer is extremely sensitive to physical properties of the 2D system. It provides a unique tool for investigating electron correlations not imposed by a magnetic field, and in-plane and out-of-plane many-electron dynamics, including short-wavelength in-plane excitations. It is also sensitive to the
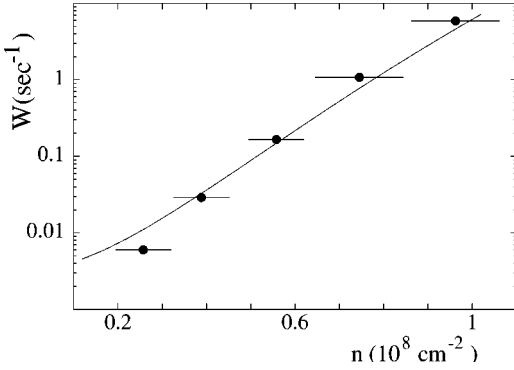
FIG. 8. The rate of electron tunneling from the helium surface W for $B=0$ as a function of the electron density. The dots show the experimental data (Ref. 5). The pulling field $\mathcal{E}_\perp$ was calculated from the geometry of the experimental cell, the applied voltage, and the density.

rates of transitions between intrawell states. There arise new physical phenomena, such as magnetic field enhanced tunneling and switching back and forth between tunneling from different intrawell states and between tunneling and activation. The effect of the field on tunneling from a correlated system depends on the interrelation between the characteristic rate of interelectron momentum exchange, the reciprocal duration of tunneling in imaginary time $1/\tau_f$, and temperature.

For low temperatures, where escape occurs via tunneling from the ground intrawell state, the tunneling rate is affected primarily by high-frequency in-plane many-electron vibrations, which are determined by short-range order in the 2DES. The vibration frequencies are of the order of the characteristic zone-boundary frequency of the Wigner crystal ω_p. If $\omega_p \gg 1/\tau_f$, the effect of the magnetic field on tunneling is nearly completely compensated in the case where the width of the tunneling barrier is small compared to the interelectron distance.

At higher temperatures, the magnetic field may in fact *enhance* rather than suppress the rate of tunneling decay. The overall escape rate as a function of B and T, and switching between different escape regimes, have been analyzed for simple but realistic models of the tunneling barrier.

Our results on the field dependence of the tunneling rate and its evolution with temperature, including field-induced tunneling enhancement, are in full qualitative and quantitative agreement with the existing experimental data on tunneling from a strongly correlated 2DES on helium,[5] with no adjustable parameters.

The results also apply to 2DES in semiconductor heterostructures. For correlated systems in semiconductors, tunneling has been investigated mostly for the magnetic field **B** perpendicular or nearly perpendicular to the electron layer, see Ref. 3. The data on tunneling in a field parallel to the layer refer to high density double-layer 2DESs (Refs. 29, 30) with a thin barrier, where the tunneling matrix element could be assumed to be nearly independent of the field.

The effect of a parallel magnetic field is most pronounced in systems with shallow and broad barriers $U(z)$, for which it has not been investigated. For example, in a GaAlAs struc-

ture with a square barrier of width $L=0.1\ \mu$m and height $\gamma^2/2m=0.02$ eV, for the electron density $n=1.5 \times 10^{10}$ cm^{-2} and $B=1.2$ T we have $\omega_p \tau_0 \approx 0.6$ and $\omega_c \tau_0 \approx 1$ ($\tau_0 = mL/\gamma$ is the tunneling duration for $n=B=0$). The results of Sec. V C for square barriers (with account taken of the correlation-hole correction) show that the interelectron momentum exchange should significantly modify the tunneling rate in this parameter range.[7] This provides a comparatively simple and direct means for revealing electron correlations, and possibly even a transition from an electron fluid to a pinned Wigner crystal.

APPENDIX: MANY-BODY WKB APPROXIMATION

1. General formulation

In this section we obtain a general expression for the escape rate W. We assume that the state of the system under the barrier can be described in the WKB approximation, but at the same time, the intrawell electron motion can be strongly quantized. Under the barrier, the interaction of the tunneling electron with phonons of the Wigner crystal is strong. One should therefore think of escape of the coupled electron-phonon system. We enumerate the states of this system ψ_α by the quantum number $\alpha=(n,\{n_{\mathbf{k}j}\})$, where n enumerates the states of quantized intrawell electron motion in the z direction, and $n_{\mathbf{k}j}$ are the phonon occupation numbers. For fast intrawell relaxation, escape is characterized by a single rate W, as explained in the text. To logarithmic accuracy

$$W = Z^{-1} \sum_\alpha W_\alpha \exp(-\beta E_\alpha),$$

$$(A1)$$

$$W_\alpha = C_\alpha \exp[-2S_\alpha(\boldsymbol{\xi}_\mathrm{f}, \boldsymbol{\xi}_\mathrm{in})] |\psi_\alpha(\boldsymbol{\xi}_\mathrm{in})|^2.$$

Here we introduced a vector $\boldsymbol{\xi} = (z, \{\mathbf{p}_{\mathbf{k}j}\})$ with components which enumerate the z-coordinate of the tunneling electron and the "coordinates" $\mathbf{p}_{\mathbf{k}j}$ of the phonons, Z is the partition function calculated neglecting escape, and C_α are the prefactors in the partial escape rates W_α, they will not be discussed in this paper.

The exponents in W_α are determined[19] by the wave functions $\psi_\alpha(\boldsymbol{\xi})$ at the turning points $\boldsymbol{\xi}_\mathrm{f}$ on the boundary of the classically accessible range ($\boldsymbol{\xi}_\mathrm{f}$ depend on α, see below). It is convenient to evaluate $\psi_\alpha(\boldsymbol{\xi}_\mathrm{f})$ in two steps, each of which gives an exponential factor. The first factor, $\exp[-S_\alpha(\boldsymbol{\xi}_\mathrm{f}, \boldsymbol{\xi}_\mathrm{in})]$, describes decay of the wave function deep under the barrier. Formally, it relates $\psi_\alpha(\boldsymbol{\xi}_\mathrm{f})$ to $\psi_\alpha(\boldsymbol{\xi}_\mathrm{in})$. The point $\boldsymbol{\xi}_\mathrm{in}$ is chosen close to the well, but it also lies under the barrier, so that S_α can be calculated in the WKB approximation. The second factor is $\psi_\alpha(\boldsymbol{\xi}_\mathrm{in})$ itself. The resulting rate should be independent of $\boldsymbol{\xi}_\mathrm{in}$.

We start with the function $S_\alpha(\boldsymbol{\xi}, \boldsymbol{\xi}_\mathrm{in})$. To the lowest order in $\hbar$, for systems with time-reversal symmetry (which we

"restored" by the canonical transformation) it is the action for a classical underbarrier motion in imaginary time $\tau = it$ with purely imaginary momenta[12]

$$p_z = i \partial S / \partial z, \quad \mathbf{u}_{\mathbf{k}j} = -i \partial S / \partial \mathbf{p}_{\mathbf{k}j}. \qquad (A2)$$

As a function of imaginary time τ, the action $S(\boldsymbol{\xi}, \boldsymbol{\xi}_{\text{in}})$ is given by the integral of the Euclidean Lagrangian L_E,

$$S_\alpha(\boldsymbol{\xi}, \boldsymbol{\xi}_{\text{in}}) = \int_0^\tau L_E d\tau - E_\alpha \tau. \qquad (A3)$$

The Lagrangian L_E is obtained from the Hamiltonian (2) using the Legendre transformation $L = p_z(dz/dt) - \Sigma \mathbf{u}_{\mathbf{k}j}(d\mathbf{p}_{\mathbf{k}j}/dt) - H$, followed by the transition to imaginary time, which gives

$$L_E = L_0 + L_v + L_B. \qquad (A4)$$

Here, $L_0 = (m/2)\dot{z}^2 + U(z)$ is the Eucledian Lagrangian for motion in the z direction, $L_B = H_B$ is the term induced by the magnetic field, and L_v is the phonon Lagrangian, $L_v = \Sigma_{\mathbf{k}j} L_{\mathbf{k}j}$, with

$$L_{\mathbf{k}j} = \frac{1}{2m} \mathbf{p}_{\mathbf{k}j} \mathbf{p}_{-\mathbf{k}j} + \frac{1}{2m \omega_{\mathbf{k}j}^2} \dot{\mathbf{p}}_{\mathbf{k}j} \dot{\mathbf{p}}_{-\mathbf{k}j} \qquad (A5)$$

(overdot means differentiation over τ).

The classical equations of motion in imaginary time have the standard form

$$\frac{d}{d\tau} \frac{\partial L_E}{\partial \dot{\boldsymbol{\xi}}} - \frac{\partial L_E}{\partial \boldsymbol{\xi}} = 0. \qquad (A6)$$

To calculate the escape rate, one has to find a trajectory which starts at $\boldsymbol{\xi}(0) = \boldsymbol{\xi}_{\text{in}}$ and reaches the boundary of the classically accessible range $\boldsymbol{\xi}_f$ at some time τ_f, and to calculate the action S_α along this trajectory.

If the potential barrier $U(z)$ is smooth, the wave function and its derivatives under the barrier have to match the WKB wave function in the classically allowed range behind the barrier. Matching occurs at a turning point of the classical motion (A6) where the derivatives of the exponents of the both wave functions become equal to zero,[19] $\partial S_\alpha / \partial z = \partial S_\alpha / \partial \mathbf{p}_{\mathbf{k}j} = 0$, i.e.,

$$\dot{z}(\tau_f) = 0, \quad \dot{\mathbf{p}}_{\mathbf{k}j}(\tau_f) = \mathbf{0}. \qquad (A7)$$

Equation (A7) is also the condition of the extremum of S_α with respect to the points $\boldsymbol{\xi}$ on the boundary of the classically accessible range: the escape rate is determined by the minimum of S_α on this boundary. A detailed analysis of the behavior of multidimensional tunneling trajectories in imaginary time for systems with time-reversal symmetry for a parabolic well is given in Ref. 31.

It follows from Eqs. (A6) and (A7) that, if the equations of motion are extended beyond τ_f, the system will bounce off the turning point and then move under the barrier back to the starting point. The section of the trajectory for $\tau > \tau_f$ is mirror symmetrical to that for $\tau < \tau_f$,

$$z(\tau_f + \tau) = z(\tau_f - \tau), \quad \mathbf{p}_{\mathbf{k}j}(\tau_f + \tau) = \mathbf{p}_{\mathbf{k}j}(\tau_f - \tau), \quad (A8)$$

where $0 \leq \tau \leq \tau_f$. The tunneling exponent $2S_\alpha$ can be calculated along the trajectory (A6) which starts at $\boldsymbol{\xi}_{\text{in}}$ and comes back to the same point in time $2\tau_f$.

For the boundary conditions (A7), the time τ_f is determined by the initial conditions on the trajectory, which are given by $\psi_\alpha(\boldsymbol{\xi}_{\text{in}})$. If the intrawell dynamics is semiclassical, the dominating contribution to the overall rate W (A1) comes from the energies E_α for which the duration of the tunneling motion $\tau_f = \beta/2$.[12] In the general case this is no longer true.

2. The wave function close to the well

We are interested in the case where the width of the quantum well is much less than the typical width L of the tunneling barrier. More precisely, we assume that for low-lying intrawell states n, the characteristic lengths $1/\gamma_n$ of localization in the z direction are $\gamma_n^{-1} \ll L$. Then, even where the effect of the magnetic field accumulates under the barrier and the tunneling rate is strongly changed, the field may still only weakly perturb the intrawell motion. In this case, inside the well and close to it, the out-of-plane electron motion is separated from the in-plane vibrations, and the state energies are

$$E_\alpha = E_n + \sum_{\mathbf{k}j} \varepsilon_{\mathbf{k}j}, \quad \varepsilon_{\mathbf{k}j} = \omega_{\mathbf{k}j} n_{\mathbf{k}j}. \qquad (A9)$$

Usually the interlevel distances $E_{n+1} - E_n \gg \omega_{\mathbf{k}j}$, for low-lying levels.

Because of the separation of motion, we can choose a plane $z = z_{\text{in}}$ under the barrier but close to the well, so that for $z \approx z_{\text{in}}$ the wave functions $\psi_\alpha(\boldsymbol{\xi})$ are semiclassical and factor,

$$\psi_{n,\{n_{\mathbf{k}j}\}}(\boldsymbol{\xi}) \propto e^{-\gamma_n z} \exp\left[-\sum_{\mathbf{k}j} S_{n_{\mathbf{k}j}}(\mathbf{p}_{\mathbf{k}j}) \right]. \qquad (A10)$$

Here, γ_n is given by Eq. (9), whereas $S_{n_{\mathbf{k}j}}$ has a standard form of the action of a free oscillator. For $\boldsymbol{\xi} = \boldsymbol{\xi}_{\text{in}}$, Eqs. (A2), (A10) give the initial velocities $\dot{\boldsymbol{\xi}}(0)$ on the WKB trajectory (A6) as functions of $\boldsymbol{\xi}(0) \equiv \boldsymbol{\xi}_{\text{in}}$.

In order to find the initial values of the phonon dynamical variables which maximize W, it is convenient to write $S_{n_{\mathbf{k}j}}$ and $\mathbf{p}_{\mathbf{k}j}$ in Eq. (A10) in the energy-phase representation, using the phonon energy $\varepsilon_{\mathbf{k}j}$ and the imaginary time $\tau_{\mathbf{k}j}$ it takes for a phonon to move under the barrier from the boundary $(2m\varepsilon_{\mathbf{k}j})^{1/2}$ of the classically allowed region to a given $\mathbf{p}_{\mathbf{k}j}$. With the Euclidean Lagrangian of the phonons (A5), we have for $\mathbf{p}_{\mathbf{k}j} = [\mathbf{p}_{\mathbf{k}j}]_{\text{in}} \equiv \mathbf{p}_{\mathbf{k}j}(0)$

$$S_{n_{\mathbf{k}j}}[\mathbf{p}_{\mathbf{k}j}(0)] = \int_{-\tau_{\mathbf{k}j}}^0 d\tau L_{\mathbf{k}j}(\tau) - \varepsilon_{\mathbf{k}j} \tau_{\mathbf{k}j} \qquad (A11)$$

and

$$\mathbf{p}_{\mathbf{k}j}(0) = \mathbf{e}_{\mathbf{k}j} (2m\varepsilon_{\mathbf{k}j})^{1/2} \cosh \omega_{\mathbf{k}j} \tau_{\mathbf{k}j},$$

$$\dot{\mathbf{p}}_{\mathbf{k}j}(0) = \mathbf{e}_{\mathbf{k}j} (2\varepsilon_{\mathbf{k}j} m \omega_{\mathbf{k}j}^2)^{1/2} \sinh \omega_{\mathbf{k}j} \tau_{\mathbf{k}j} \qquad (A12)$$

[$\mathbf{e}_{\mathbf{k}j}$ is the polarization vector of the mode $(\mathbf{k}, j)$].

3. A three-segment optimal trajectory

To evaluate the escape rate W to logarithmic accuracy, one can, following Feynman's procedure, solve the equations of motion (A6) for the vibration "coordinates" $\mathbf{p}_{\mathbf{k}j}(\tau)$ in terms of $z(\tau)$ and the initial energies $\varepsilon_{\mathbf{k}j}$ and phases $\omega_{\mathbf{k}j}\tau_{\mathbf{k}j}$. Then, from the boundary condition (A7), one can find $\tau_{\mathbf{k}j}$ and then perform thermal averaging by summing the escape rate over $n_{\mathbf{k}j}$ with the Boltzmann weighting factor. Here we give an alternative derivation, which provides a better insight into the structure of the tunneling trajectory.

We note that, from Eqs. (A1), (A3), (A10), and (A11), the partial escape rate W_α can be written as $W_\alpha \propto \exp(-R_\alpha)$, with

$$R_\alpha = \sum_{\mathbf{k}j} \int_{-\tau_{\mathbf{k}j}}^0 d\tau \, L_{\mathbf{k}j}(\tau) + \int_0^{2\tau_f} d\tau \, L_{\mathrm{E}}(\tau)$$
$$+ \sum_{\mathbf{k}j} \int_{2\tau_f}^{2\tau_f+\tau_{\mathbf{k}j}} d\tau \, L_{\mathbf{k}j}(\tau) - 2E_n \tau_f - 2 \sum_{\mathbf{k}j} \varepsilon_{\mathbf{k}j}(\tau_f + \tau_{\mathbf{k}j})$$

$$(A13)$$

[the term $\gamma_n z_{\mathrm{in}}$ in Eq. (A10) is small compared to $R_\alpha \sim \gamma_n L$ and should be incorporated into the prefactor, see Sec. VI].

From Eq. (A13), the tunneling electron in its nth state, accompanied by phonons, move under the barrier along a classical trajectory for the imaginary time $2\tau_f$. This motion is described by the Lagrangian L_{E}. Before and after that, the phonons are moving on their own, disconnected from the electronic z motion, for times $\tau_{\mathbf{k}j}$ and with the Lagrangian $L_v = \Sigma_{\mathbf{k}j} L_{\mathbf{k}j}$, so that the overall phonon trajectories make closed loops which start and end at turning points.

In the WKB approximation, the sum of W_α (A1) over the phonon occupation numbers $n_{\mathbf{k}j}$ can be replaced by the integral over $\varepsilon_{\mathbf{k}j}$, which should then be evaluated by the steepest descent method. The corrections due to the discreteness of the values of $\varepsilon_{\mathbf{k}j}$ are small provided $\omega_{\mathbf{k}j}\tau_f \ll R_\alpha$. From Eq. (A13), the extremum of $\exp(-R_\alpha - \beta E_\alpha)$ with respect to $\varepsilon_{\mathbf{k}j}$ is reached for

$$\tau_{\mathbf{k}j} = \frac{1}{2}\beta - \tau_f. \qquad (A14)$$

This expression shows that the duration of the free phonon motion $\tau_{\mathbf{k}j}$ is the same for all vibrational modes. Moreover, the overall duration of the three-segment optimal trajectory of each vibration is $2(\tau_{\mathbf{k}j} + \tau_f) = \beta$. Examples of the trajectories are shown in Fig. 9.

For low temperatures, $\beta > 2\tau_f$, the direction of time along the vibrational trajectory does not change, $\tau_{\mathbf{k}j} > 0$. The corresponding branch of the intrawell vibrational wave function (A10) $\propto \exp\{-S_{n_{\mathbf{k}j}}[\mathbf{p}_{\mathbf{k}j}(0)]\}$ decays with the increasing
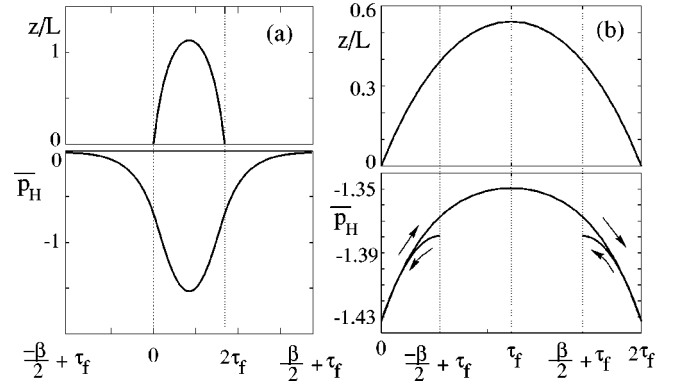

FIG. 9. Optimal trajectories of the tunneling electron $z(\tau)$ and the vibrations of the WC for $\beta > 2\tau_f$ (a) and $\beta < 2\tau_f$ (b). The numerical data refer to the Einstein model of the Wigner crystal, with $\overline{p_H}$ being the vibrational momentum in the Hall direction $\hat{\mathbf{z}} \times \mathbf{B}$, in units $\hbar\gamma_g/2$ (γ_g is the value of γ_n in the ground state $n=1$). The arrows show the direction of motion along the optimal trajectory when $\beta < 2\tau_f$. The tunneling potential is of the form (16), with dimensionless cyclotron frequency $\omega_c \tau_0 = 2.0$, where $\tau_0 = 2mL/\gamma_g$ is the imaginary tunneling time for $B=0$. The vibrational frequency is $\omega_p \tau_0 = 1.0$.

$|\mathbf{p}_{\mathbf{k}j}(0)|$ in the classically forbidden region $|\mathbf{p}_{\mathbf{k}j}(0)| > (2m\varepsilon_{\mathbf{k}j})^{1/2}$. In contrast, for $\beta < 2\tau_f$, we have $\tau_{\mathbf{k}j} < 0$. This shows that the extremum over $\varepsilon_{\mathbf{k}j}$ is reached if the intrawell vibrational wave function is analytically continued from the decaying to the increasing branch.

For $\tau_{\mathbf{k}j} = (\beta/2) - \tau_f < 0$, the "free-vibrations" term $S_{n_{\mathbf{k}j}}$ is negative, it gives rise to the decrease of the tunneling exponent. This is the formal reason why, for sufficiently high temperatures, an in-plane magnetic field can increase the tunneling rate compared to its $B=0$ value by coupling thermally-excited in-plane vibrations to the tunneling motion.

If the intrawell motion transverse to the layer were semiclassical, the sum over the energy levels of this motion E_n in Eq. (A1) could be replaced by an integral. The extremum of the integrand is reached for $\tau_f = \beta/2, \tau_{\mathbf{k}j} = 0$. This is the familiar result of the instanton theory, in which the whole system moves under the barrier from the well to the turning point and back over the imaginary time β.[12] Clearly, in this case one should not expect the tunneling rate to be enhanced by a magnetic field.

In the case of 2D electron systems, the potential well is *not* parabolic, and each term in the sum over n (A1) has to be considered separately. Except for narrow parameter intervals, the contribution of one of them is dominating, and the electron tunnels from the corresponding state.

---

*Email address: dykman@pa.msu.edu

[1] E. Abrahams, S.V. Kravchenko, and M.P. Sarachik, Rev. Mod. Phys. **73**, 251 (2001).

[2] *Two-dimensional Electron Systems on Helium and Other Cryogenic Substrates*, edited by E. Andrei (Kluwer, New York 1997).

[3] Presumably, correlations played a very substantial role in the gi-

ant increase of inter-layer tunneling observed recently in double layer heterostructures by I.B. Spielman, J.P. Eisenstein, L.N. Pfeiffer, and K.W. West, Phys. Rev. Lett. **84**, 5808 (2000).

[4] *Perspectives in Quantum Hall Effects*, edited by S. Das Sarma and A. Pinczuk (Wiley, New York, 1997).

[5] L. Menna, S. Yücel, and E.Y. Andrei, Phys. Rev. Lett. **70**, 2154

(1993); E.Y. Andrei, in *Two-dimensional Electron Systems on Helium and Other Cryogenic Substrates* (Ref. 2), p. 207.

[6] T. Barabash-Sharpee, M.I. Dykman, and P.M. Platzman, Phys. Rev. Lett. **84**, 2227 (2000).

[7] M.I. Dykman, T. Sharpee, and P.M. Platzman, Phys. Rev. Lett. **86**, 2408 (2001).

[8] A strong effect on tunneling of the momentum transfer to defects was first discussed by B.I. Shklovskii, JETP Lett. **36**, 51 (1982); B.I. Shklovskii and A.L. Efros, Sov. Phys. JETP **57**, 470 (1983).

[9] I. Affleck, Phys. Rev. Lett. **46**, 388 (1980).

[10] A.I. Larkin and Yu.N. Ovchinnikov, Pis'ma Zh. Éksp. Teor. Fiz. **37**, 322 (1983) [JETP Lett. **37**, 382 (1983)]; J. Stat. Phys. **41**, 425 (1985).

[11] For a potential of a special form, the instanton technique was applied to tunneling of an electron coupled to harmonic oscillators in a magnetic field by P. Ao, Phys. Rev. Lett. **72**, 1898 (1994); Physica B **194-196**, 1233 (1994).

[12] J.S. Langer, Ann. Phys. (N.Y.) **41**, 108 (1967); S. Coleman, Phys. Rev. D **15**, 2929 (1977).

[13] A.O. Caldeira and A.J. Leggett, Ann. Phys. (N.Y.) **149**, 374 (1983).

[14] T. Sharpee, M.I. Dykman, and P.M. Platzman, cond-mat/0106566 (unpublished).

[15] C.C. Grimes aand G. Adams, Phys. Rev. Lett. **42**, 795 (1979).

[16] D.S. Fisher, B.I. Halperin, and P.M. Platzman, Phys. Rev. Lett. **42**, 798 (1979).

[17] M.Ya. Azbel and P.M. Platzman, Phys. Rev. Lett. **65**, 1376 (1990).

[18] R. P. Feynman and A. R. Hibbs, *Quantum Mechanics and Path Integrals* (McGraw-Hill, New York, 1965).

[19] L.D. Landau and E.M. Lifshitz, *Quantum Mechanics: Non-relativistic Theory* (Pergamon, New York, 1977); M.V. Berry and K.E. Mount, Rep. Prog. Phys. **35**, 315 (1972).

[20] R. Landauer and Th. Martin, Rev. Mod. Phys. **66**, 217 (1994).

[21] A.J. Leggett, S. Chakravarty, A.T. Dorsey, M.P.A. Fisher, A. Garg, and W. Zwerger, Rev. Mod. Phys. **59**, 1 (1987).

[22] For $B=0$, a good agreement between measured and numerically evaluated tunneling rates for electrons on helium was obtained by G.F. Saville, J.M. Goodkind, and P.M. Platzman, Phys. Rev. Lett. **70**, 1517 (1993).

[23] M.J. Lea, P. Fozooni, A. Kristensen, P. J. Richardson, K. Djerfi, M. I. Dykman, C. Fang-Yen, and A. Blackburn, Phys. Rev. B **55**, 16 280 (1997).

[24] Y. Iye, K. Kono, K. Kajita, and W. Sasaki, J. Low Temp. Phys. **38**, 293 (1980).

[25] M.I. Dykman, J. Phys. C **16**, 7397 (1982).

[26] S. Nagano, S. Ichimaru, H. Totsuji, and N. Itoh, Phys. Rev. B **19**, 2449 (1979).

[27] The rate of activation escape may depend on the magnetic field. The field "pushes" the ground state upward in energy, by $m\omega_c^2[\langle z^2\rangle - \langle z\rangle^2]/2$, for a weak field (the averaging is performed for the ground state). It also changes the wave functions with energies close to the barrier top. For example, for $B = 0.4$ T the magnetic length $l = (\hbar c/eB)^{1/2}$ is ~ 0.6 of the distance from the helium surface to the barrier top position $(\Lambda/|e\mathcal{E}_\perp|)^{1/2}$.

[28] R.J. Price, Proc. Phys. Soc. London **67**, 383 (1954).

[29] J.P. Eisenstein, T.J. Gramila, L.N. Preiffer, and K.W. West, Phys. Rev. B **44**, 6511 (1991); S.Q. Murphy, J.P. Eisenstein, L.N. Preiffer, and K.W. West, *ibid.* **52**, 14 825 (1995).

[30] J. Smoliner, W. Demmerle, G. Berthold, E. Gornik, G. Weimann, and W. Schlapp, Phys. Rev. Lett. **63**, 2116 (1989); G. Rainer, J. Smoliner, E. Gornik, G. Böhm, and G. Weimann, Phys. Rev. B **51**, 17 642 (1995).

[31] U. Eckern and A. Schmid, in *Quantum Tunnelling in Condensed Matter*, edited by Yu. Kagan and A.J. Leggett (Elsevier, New York, 1992), p. 145.